Original Research article

Sulfate Sulfuric Acid (SUSA)/NaNO₂: Efficient Procedure for *N*-Nitrosation of Secondary Amines and DFT Studies of the Products

Lotfi Shiri[a] *, Davood Sheikh[b], Sakineh Janinia[a], Masoome Sheikhi[c]

[a] Department of Chemistry, Faculty of Science, Ilam University, P.O. Box 69315516, Ilam, Iran

[b] Young Researchers & Elite Club, Hamedan Branch, Islamic Azad University, Hamedan, Iran

[c] Young Researchers & Elite Club, Gorgan Branch, Islamic Azad University, Gorgan, Iran
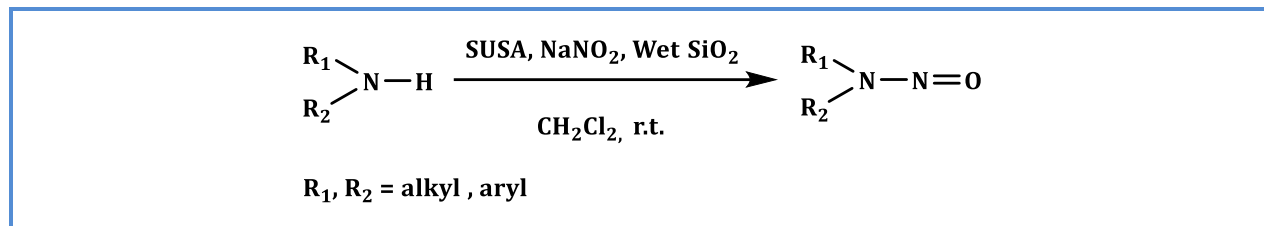
ABSTRACT

We present the preparation and characterization of sulfate sulfuric acid (SUSA) for the first time. The SUSA showed the best activity in efficient nitrosation of secondary amines under mild condition with excellent yields. Sulfate sulfuric acid (SUSA), is a safe, stable and recyclable solid acid and is a suitable reagent for many organic reactions. The quantum theoretical calculations for products (**2a-j**) were performed by density functional theory (DFT/B3LYP/6-31+G*). Natural charge, frontier molecular orbitals (FMOs), total density of states (DOS), molecular electrostatic potential (MEP) and NBO analysis of the products were investigated by theoretical calculations. Also, molecular properties such as ionisation potential (I), electron affinity (A), chemical hardness (η), electronic chemical potential (μ) and electrophilicity (ω) were obtained for products.

Corresponding author: E-mail: lshiri47@yahoo.com
Department of Chemistry, Faculty of Science, Ilam University, P.O. Box 69315516, Ilam, Iran
Tel: +98841 222 7022, Fax: +98841 222 7022

Graphical Abstract

$$R_1,R_2 \quad N-H \xrightarrow[\text{CH}_2\text{Cl}_2, \text{ r.t.}]{\text{SUSA, NaNO}_2, \text{ Wet SiO}_2} R_1,R_2 \quad N-N=O$$
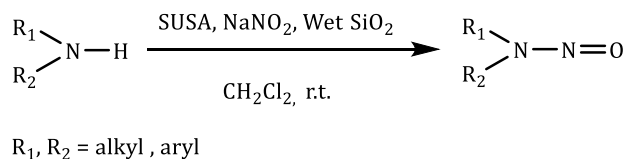
R_1, R_2 = alkyl , aryl

Introduction

N-nitrosamines are important organic compounds because of their pharmaceutical applications [1, 2]. These compounds have been used as antioxidants, lubricant additives and pesticides [3] and are useful synthetic intermediates in preparation of various N-N bonded functionalities [4].

N-nitrosation of amines is an important reaction in organic synthesis. Different nitrosating agents as sources of nitrosonium ions including nitrous acid, nitrosyl chloride, dinitrogen trioxide and alkyl nitrites have been applied widely [5]. Other efficient nitrosating agents such as Mukaiyama reagent/NaNO₂/wet SiO₂ [6], nafion-H®/NaNO₂ [7], trichloromelamine/NaNO₂ [8], PVP-N₂O₄ [9], Ionic liquid [10], PBBS or TBBDA with sodium nitrite have also been used [11]. The reported methods show different degrees of successes as well as limitations such as harsh reaction conditions, expensive catalyst/reagent, toxic organic solvents, low product yields, long reaction times.

Today, heterogenation of chemical systems is an active field in industrial and laboratorial chemistry because of simplification in handling procedures, reduction of corrosion, green chemistry point of view, easy and clean reaction and simple work-up. With regards to wide application of acids as reagent or catalyst in organic chemistry, introduction of new in organic solid acid can be useful in this direction [12]. In recent years, computational chemistry has become an important tool for chemists and a well-accepted partner for experimental chemistry [13-15]. In continuation of our research and interest in the development of novel synthetic methodologies and computational chemistry [16-20] we now report SUSA/NaNO₂/wet SiO₂ as a new mixed reagent system for the generation of nitrosonium ions under mild and efficient reaction conditions (Scheme 1).

$$R_1,R_2 \quad N-H \xrightarrow[\text{CH}_2\text{Cl}_2, \text{ r.t.}]{\text{SUSA, NaNO}_2, \text{ Wet SiO}_2} R_1,R_2 \quad N-N=O$$

R_1, R_2 = alkyl , aryl

Scheme 1. *N*-nitrosation of amines using sulfate sulfuric acid (SUSA)/NaNO₂/wet SiO₂

Experimental

Material and Methods

Materials were prepared from Fluka and Merck companies and utilized without purification. Melting points were measured on a SMPI apparatus. The solvent was evaporated by Rotavapor IKA R-300. IR (KBr) spectra were recorded on a Shimadzu 470 and PerkinElmer 781 spectrophotometer. In this work, we have carried out quantum theoretical calculations for **2a-j** using B3LYP/6-31+G* level (DFT) [21]. At first, we have optimized structures using Gaussian 03W program package [22] (see Figure 1 and 2). The electronic properties such as E_{HOMO}, E_{LUMO}, HOMO-LUMO energy gap (ΔE), E_{HOMO-1}, E_{LUMO+1}, natural charges, molecular properties, dipole moment (μ_D) and point group were detected. The optimized molecular structure, HOMO and LUMO surfaces were visualized using Gauss View 03 program [23]. The electronic structure of **2a-j** was studied by using natural bond orbital (NBO) analysis at the same level in order to understand various second-order interactions between the filled orbitals of one subsystem and vacant orbitals of another subsystem, which is a measure of the inter-molecular delocalization or hyper conjugation.

Typical procedure for the synthesis of SUSA

To a round bottom flask equipped with ice-bath containing 0.2 mol chlorosulfonic acid (23.30 g), 0.1 mol (14.20 g) anhydrous sodium sulfate was added gradually. Then the mixture was shaken for 60 min. SUSA as white solid was obtained. The prepared catalyst was characterized by determination of physical data and FT-IR spectrum. The overlaid FT-IR spectra of sodium sulfate and sulfate sulfuric acid (SUSA) are shown in Figure 1.
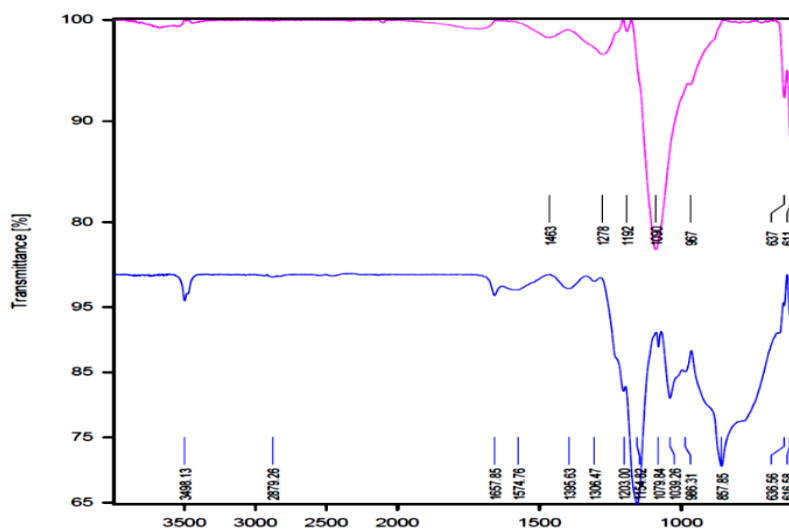

Figure 1. Overlaid FT-IR spectra of Na_2SO_4 and $H_3OSO(SO_2)$, OSO_3H (SSA)

Physical and spectroscopic data of SUSA: white solid, m.p= 204-205 °C, IR (KBr) ν_{max}/cm^{-1}: 3498 (OH), 1203–1154 (S = O), 1039 (S-O).

General procedure for the *N*-nitrosation of secondary amines

To a solution of secondary amine (1 mmol) in 5 mL dichloromethane, 2 mmol $NaNO_2$, 0.3 mmol wet SiO_2 and 1 mmol SUSA were added. The reaction mixture was stirred at 25 °C for appropriate time (Table 2). The progress of reaction was checked by TLC. Upon completion, sulfate sodium (1.5 mmol) was subjoined to the reaction mixture and continue the stirring for 20 minutes. The mixture was filtered off. The solvent was vaporized and pure *N*-nitroso amine is produced. All the synthesized compounds were confirmed by comparing their physical and spectral data found in the literature. Physical and spectroscopic data of product 2 as given below:

Pale yellow solid, m.p: 57-58 °C. IR (KBr) ν_{max}/cm^{-1}: 3085-3064 (arom. CH), 3000-2979 (aliph. CH), 1600, 1585, and 1495 (arom. C=C), 1455 (N=O), 1316 (C-N), 1071 (N-N); ^{1}H NMR (CDCl$_3$) δ/ppm: 4.64 (s, 2H, CH$_2$), 5.18 (s, 2H, CH$_2$), 7.23-7.43 (m, 10H, Ar-H).

Result and Discussion

In order to establish the conditions of the titled reactions, we preliminary examined the model reaction for syntheses of *N*-nitrosodibenzylamine as test compounds. Various parameters such as the amount of SUSA, $NaNO_2$, influence of wet SiO_2 and nature of the solvent, were investigated.

Effect of amount of SUSA on the synthesis of *N*-nitrosodibenzylamine

The effect of amount of SUSA on the synthesis of *N*-nitrosodibenzylamine has been investigated, and the results are summarized in Table 1. As seen in this table, the best result in terms of the reaction time and yield was obtained when the reaction was conducted using 10 mol% SUSA (entry 3).

Table 1. Effect of SUSA on the synthesis of *N*-nitrosodibenzylamine
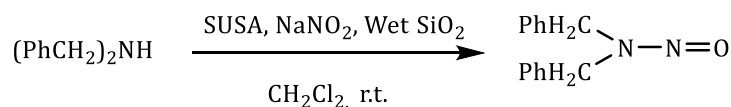
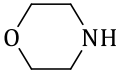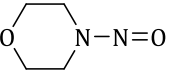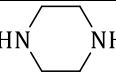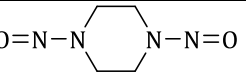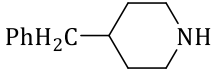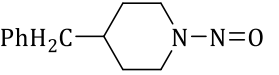| Entry	SUSA (mmol)	Time (min)	Yield (%)[a]
1	0.25	60	Trace
2	0.5	60	90
3	1	2	92

[a] Isolated yields

Effect of solvent on the synthesis of *N*-nitrosodibenzylamine

To achieve suitable reaction conditions in terms of reaction time and yield, various solvents such as EtOH, Et$_2$O, MeCN, CHCl$_3$ and CH$_2$Cl$_2$ were investigated. The reaction gives the highest yield of the corresponding *N*-nitoso compounds in CH$_2$Cl$_2$.

To estimate the influence of wet SiO$_2$ in this research, we performed the synthesis of *N*-nitrosodibenzylamine with SUSA/NaNO$_2$ without using wet SiO$_2$. The reaction did not progress after 180 min stirring.

To show the applicability and generality of this procedure, we have examined the reaction of various secondary amines with SUSA, NaNO$_2$ and wet SiO$_2$ in stirring dichloromethane. The results are tabulated in Table 2. As indicated in this table, varieties of secondary amines are converted to the *N*-nitroso amines in excellent yield under optimum reactions condition (Table 2, entries a-j).
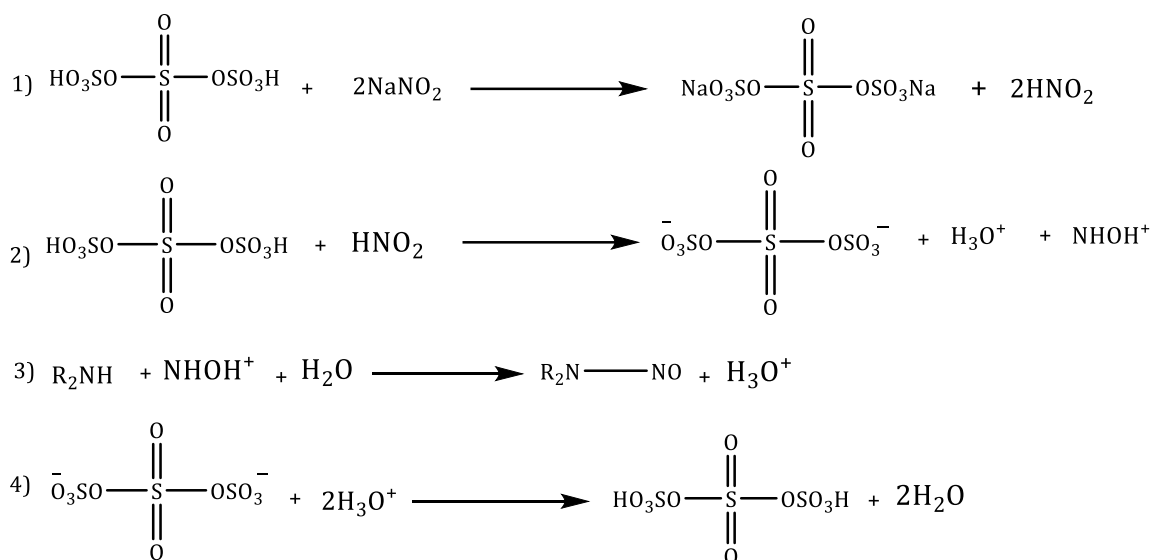
Table 2. Synthesis of various *N*-nitroso amines with sodium nitrite/SUSA[a]

Entry	Substrate 1	Product 2	Time (min)	Yield (%)a
a	(PhCH$_2$)$_2$NH	(H$_2$CPh)$_2$N N O	2	92
b	(CH$_3$)$_3$C(PhCH$_2$)NH	(H$_3$C)$_3$C(PhH$_2$C)N N O	1	98
c	O⟨ ⟩NH	O⟨ ⟩N−N=O	1	95
d	NH(CH$_2$Ph)CH$_2$CH$_3$	H$_3$CH$_2$C(PhH$_2$C)NNO	2	91
e	HN⟨ ⟩NH	O=N−N⟨ ⟩N−N=O	2	98
f	(C$_6$H$_{11}$)CH$_3$NH	(C$_6$H$_{11}$)H$_3$CNNO	15	95
g	PhH$_2$C−⟨ ⟩NH	PhH$_2$C−⟨ ⟩N−N=O	6	99
h	(*i-Pr*)$_2$NH	(-*iPr*)$_2$NNO	4	96
i	NH(C$_6$H$_{13}$)$_2$	(C$_6$H$_{13}$)$_2$NNO	3	99
j	(*i-Pr*)(PhCH$_2$)NH	(*i-Pr*)(PhH$_2$C)NNO	2	97

[a] secondary amines (1 mmol), SUSA (1mmol), NaNO$_2$ (2 mmol), Wet SiO$_2$ (0.3 mmol), dichloromethane (5 mL), stirring at r.t.
[b] Isolated yields

A possible mechanism that explains the formation of products **2a-j** is shown in Scheme 2.

1) $HO_3SO-\overset{\overset{\displaystyle O}{\|}}{\underset{\underset{\displaystyle O}{\|}}{S}}-OSO_3H$ + $2NaNO_2$ $\longrightarrow$ $NaO_3SO-\overset{\overset{\displaystyle O}{\|}}{\underset{\underset{\displaystyle O}{\|}}{S}}-OSO_3Na$ + $2HNO_2$

2) $HO_3SO-\overset{\overset{\displaystyle O}{\|}}{\underset{\underset{\displaystyle O}{\|}}{S}}-OSO_3H$ + HNO_2 $\longrightarrow$ $^-O_3SO-\overset{\overset{\displaystyle O}{\|}}{\underset{\underset{\displaystyle O}{\|}}{S}}-OSO_3^-$ + H_3O^+ + $NHOH^+$

3) R_2NH + $NHOH^+$ + H_2O $\longrightarrow$ R_2N-NO + H_3O^+

4) $^-O_3SO-\overset{\overset{\displaystyle O}{\|}}{\underset{\underset{\displaystyle O}{\|}}{S}}-OSO_3^-$ + $2H_3O^+$ $\longrightarrow$ $HO_3SO-\overset{\overset{\displaystyle O}{\|}}{\underset{\underset{\displaystyle O}{\|}}{S}}-OSO_3H$ + $2H_2O$

Scheme 2. Plausible mechanism for synthesis of various *N*-nitroso amines

To show the advantage and drawbacks of this method, we have compared some of our outcome with various catalytic systems were reported (Table 3). As indicated in the Table 3, SUSA in comparison with other reagents performs this alteration in shorter reaction times and milder reaction condition.

Table 3. Synthesis of *N*-nitrosodibenzylamine by SUSA in comparison with other reagents

Entry	Nitrosating agent	Condition (°C)	Time (min)	Yield (%)[a]	References
1	SUSA/ NaNO₂	r.t	2	92	This work
2	IL-ONO	0-25°C	65	97	10
3	Trichloromelamine–NaNO₂	r.t	15	92	8
4	Molybdatophosphoric acid/NaNO₂	r.t	20	89	6
5	Nafion-H®/NaNO₂	r.t	30	90	7
6	PBBS /NaNO₂	r.t	5	96	11

Atomic charge

The optimized structure of **2a-j** has been calculated by DFT (B3LYP/6-31+G*). We obtained the charge distributions for equilibrium geometry of **2a-j** by NBO method (natural charge) [24] using B3LYP/6-31+G* level. The total charge of the investigated molecules is equal to zero. As shown in Figure 2 and 3, all hydrogen atoms in **2a-j** have positive charge and all carbon atoms bear negative charges other than carbon of tert-butyl in **2b**. The highest values of negative charge are observed for carbon atoms in methyl groups. Also oxygen atoms in all molecules have high negative charge. In N=O group, oxygen atom has the high electronegativity rather than nitrogen. As shown in Figure 2 and 3, the nitrogen atom in N=O group has positive charge, while other nitrogen atom in molecules has negative charge.
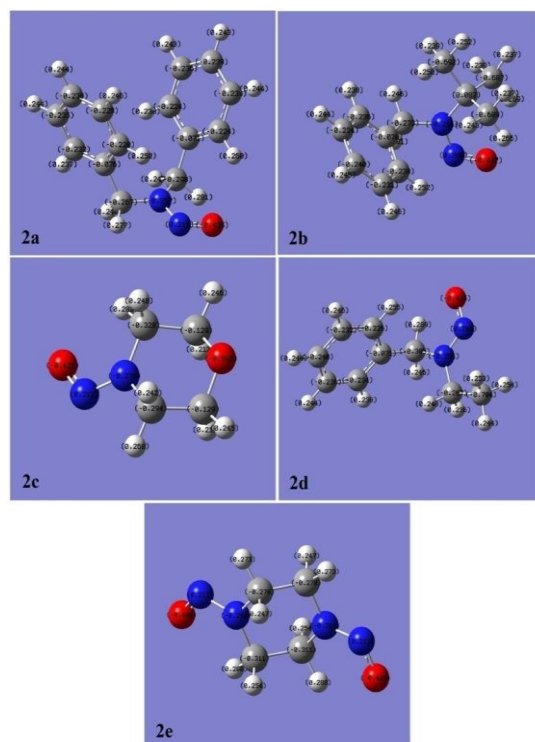
Figure 2. Geometrical structure of **2a-e** (optimized at B3LYP/6-31+G* level) and calculated natural charges (NBO) of the atoms of **2a-e**
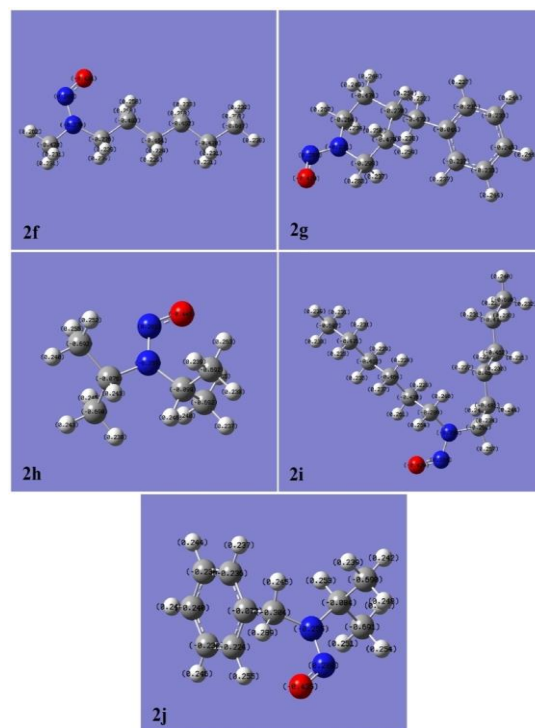

Figure 3. Geometrical structure of **2f-j** (optimized at B3LYP/6-31+G* level) and calculated natural charges (NBO) of the atoms of **2f-j**

Electronic properties

Quantum chemical methods are important to obtain information about molecular structure and electrochemical behavior. The frontier molecular orbitals (FMO) analysis calculated for **2a-j** using B3LYP/6-31+G* level [25]. The results of FMO such as E_{HOMO}, E_{HOMO-1}, E_{LUMO}, E_{LUMO+1} and HOMO-LUMO energy gap (ΔE) of **2a-j** are summarized in Table 4. The highest occupied molecular orbital (HOMO) and lowest unoccupied molecular orbital (LUMO) are the most important orbitals in a molecule. HOMO can act as an electron donor and the LUMO can act as the electron acceptor. On the other hand, LUMO can accept electrons and the LUMO energy is directly related to electron affinity [26]. A higher E_{HOMO} for the molecule indicates a higher electron-donating ability to an appropriate acceptor molecule with a low-energy empty molecular orbital [27]. The graphic pictures of HOMO and LUMO orbitals show HOMO orbital of molecules is localized mainly on N-N=O group. As shown in Figure 4 and 5, charge transfer is taking place within molecules. The HOMO→LUMO transition in **2a**, **2b**, **2d**, **2f** and **2j** implies an electron density transfer from N-N=O group to phenyl ring and LUMO orbital is focused mainly on phenyl rings. The calculated values of the HOMO–LUMO energy gap (ΔE) for molecules is listed in Table 4 and it clearly is shown in DOS plots [28]. A molecule with a small gap is more polarized and is known as soft molecule, while hard system has a big gap and is relatively small and much less polarizable [29]. A detail of quantum molecular descriptors of **2a-j** is summarized in Table 4. The is ionization potential ($I = -E_{HOMO}$) and A is electron affinity ($A = -E_{LUMO}$) [31]. Large values of electron affinity in **2e** confirm that it prefers to accept more number of electrons. Homo orbital is most heavily concentrated on N-N=O, meaning that electrophilic attack will likely occur here. The chemical hardness ($\eta = (I - A)/2$) is important property to measure the molecular stability and reactivity [31]. A hard molecule has a large energy gap (ΔE) and a soft molecule has a small energy gap (ΔE) [27]. The chemical hardness (η) values is shown that **2c** has the highest value (5.16 eV) therefore it is hard and less reactive molecule rather than other structures, while **2b** has the lowest value (4.94 eV) therefore it is soft and more reactive molecule. The electronic chemical potential ($\mu = -(I + A)/2$) is a form of the potential energy [32]. The chemical potential of the compounds is negative which it means that the compounds are stable. The μ value of **2e** is the most negative value (-4.33 eV) and **2h** is the low negative energy (-3.5 eV), therefore. The electrophilicity parameter (ω) show the stabilization in energy when the system acquires an additional electronic charge from the environment [33]. The electrophilicity index ($\omega = \mu^2/2\eta$) contains information about both electron transfer (chemical potential) and stability (hardness) and is a better descriptor of global chemical reactivity [34]. The high value of electrophilicity index shows the high capacity of the molecule to accept electrons. The structure **2e** has the highest

electrophilicity index (3.76 eV), therefore it has high capacity for acceptance electrons. Dipole moment (μ_D) is a good measure for the asymmetric nature of a structure [35]. The size of the dipole moment depends on the composition and dimensionality of the 3D structures. As shown in Table 4, structure **2g** has the highest value of dipole moment (4.9552 Debye) which refers high asymmetry in the structure and irregularly arranged which gives rise to the increased dipole moment, while structure **2e** has the highest value of dipole moment (1.6069 Debye) which refers high symmetry in the structure. Also point group of all structures is C1.

Table 4. Molecular properties of **2a-j** calculated using DFT (B3LYP/6-31+G*)

|	E_{HOMO} (eV)	E_{LUMO} (eV)	E_{HOMO-1} (eV)	E_{LUMO+1} (eV)	ΔE (eV)	I (eV)	A (eV)	μ (eV)	η (eV)	ω (eV)	μ_D (Debye)	Point group
2a	-6.45	-1.4	-6.92	-0.79	5.05	6.45	1.4	-3.92	2.52	3.05	4.1939	C1
2b	-6.17	-1.23	-7.02	-0.71	4.94	6.17	1.23	-3.7	2.47	2.77	4.2406	C1
2c	-6.57	-1.41	-7.2	0.12	5.16	6.57	1.41	-3.99	2.58	3.08	3.1585	C1
2d	-6.29	-1.22	-7.08	-0.7	5.07	6.29	1.22	-3.75	2.53	2.78	4.2680	C1
2e	-6.82	-1.84	-7.0	-1.62	4.98	6.82	1.84	-4.33	2.49	3.76	1.6069	C1
2f	-6.16	-1.09	-7.19	-0.17	5.07	6.16	1.09	-3.62	2.53	2.59	4.2635	C1
2g	-6.3	-1.16	-6.96	-0.66	5.14	6.3	1.16	-3.73	2.57	2.71	4.9552	C1
2h	-6.01	-0.99	-7.1	-0.21	5.02	6.01	0.99	-3.5	2.51	2.44	4.4438	C1
2i	-6.27	-1.13	-7.15	0.01	5.14	6.27	1.13	-3.7	2.57	2.66	4.5732	C1
2j	-6.25	-1.23	-7.05	-0.71	5.02	6.25	1.23	-3.74	2.51	2.79	4.3478	C1
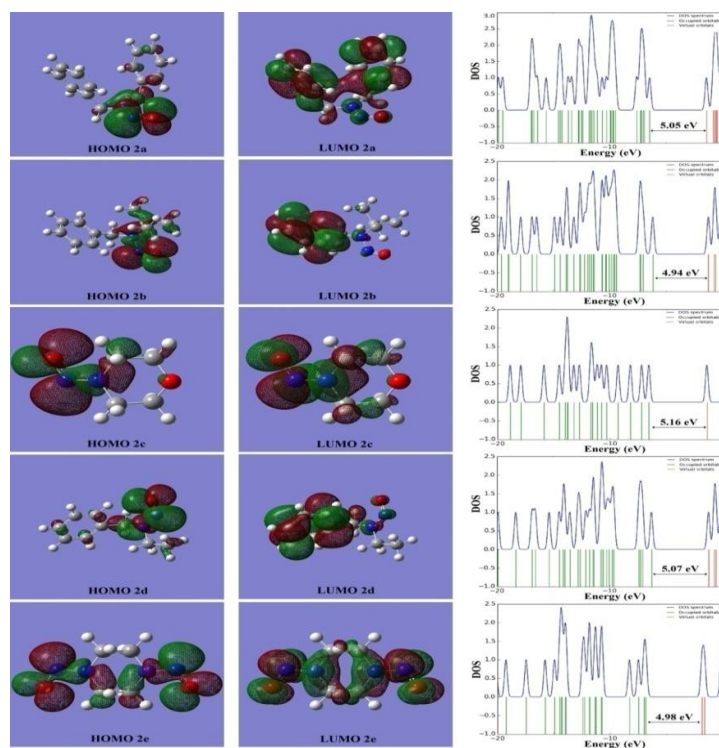
Figure 4. Calculated frontier molecular orbitals of **2a-e** and calculated DOS plots of **2a-e** (using B3LYP/6-31+G*)
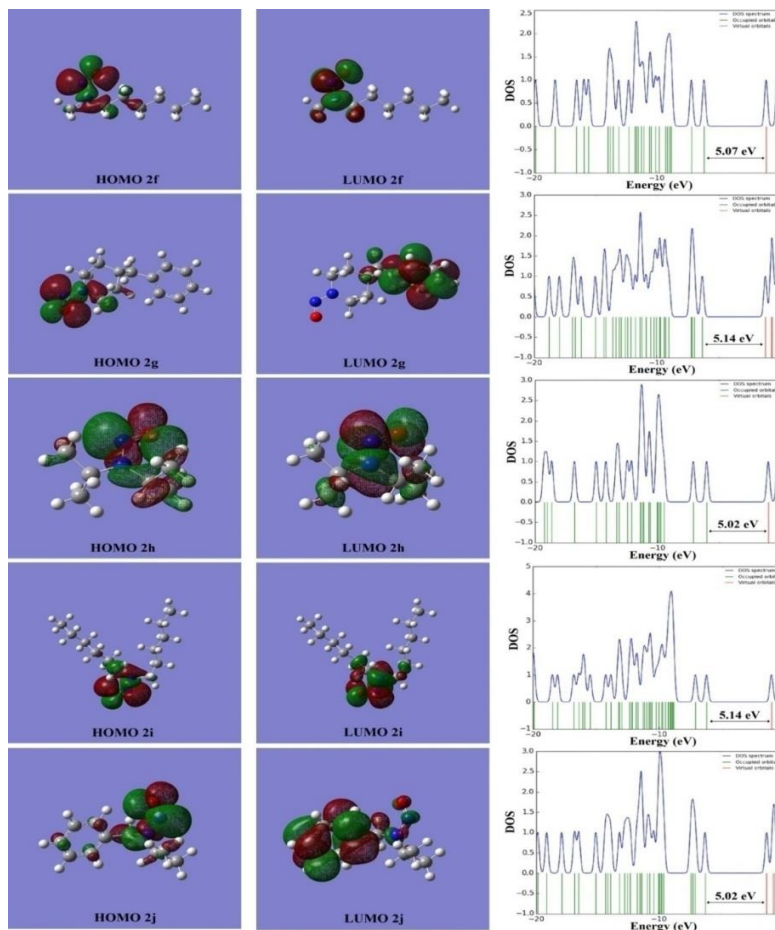
Figure 5. Calculated frontier molecular orbitals of **2f-j** and calculated DOS plots of structures **2f-j** (using B3LYP/6-31+G*)

Molecular electrostatic potential (MEP)

Molecular electrostatic potential is a graphic model that shows the electronic density. This methodology is used to investigate the electronic distribution in molecules and to evaluate the electronic distribution around molecular surfaces for compounds. To predict reactive sites of electrophilic and nucleophilic attacks for **2a-j**, MEP was checked out by theoretical calculations using B3LYP/6-31+G* level. The negative regions (red, orange and yellow color) of MEP were related to electrophilic reactivity, the positive regions (blue color) to nucleophilic reactivity and green color is neutral regions [36]. As shown in Figure 6, MEP of molecules **2c**, **2e**, **2f**, **2h** and **2i**, it is evident that the negative charge covers oxygen atom of N=O group, while negative region of molecules **2a**, **2b**, **2d**, **2g** and **2j** is mainly focused on oxygen atom of N=O group and carbon atoms of phenyl group. The positive region (blue color) is over the hydrogen atoms of CH_2 group close to N-N=O group.
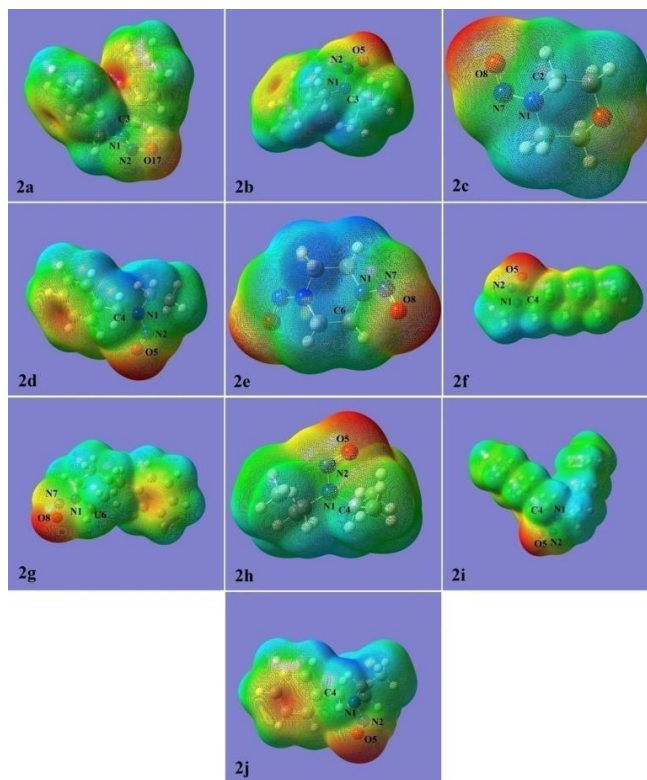
Figure 6. Molecular electrostatic potential (MEP) maps of **2a-j** calculated using B3LYP/6-31+G* level

NBO analysis

Natural bond orbital (NBO) analysis is important method for studying intra and inter-molecular bonding and interaction between bonds [37]. The results of NBO analysis such as the occupation numbers with their energies for the interacting NBOs [interaction between natural bond orbital A and natural bond orbital B (A-B)] and the polarization coefficient amounts of atoms for N-N=O group in **2a-j** are presented using the B3LYP/6-31+G* level is summarized in Table 5. (Atoms labeling is according to Figure 6). The size of polarization coefficients shows the importance of the two hybrids in the formation of the bond. The larger differences in electronegativity of the atoms involved in the bond formation are reflected in the larger differences in the polarization coefficients of the atoms [38]. According to calculated bonding orbital for the N-O bonds [BD(1)N-O and BD(2)N-O] of **2a-j**, polarization coefficients of O atoms are the higher than N atoms, which it shows importance of O atom in forming N-O bond rather than N atom. Also BD(1)N-O has high occupancy and energy rather than BD(2)N-O. BD(1)N-O represents that a single bond is formed between the N atom and O atom and BD(2)N_{21}-C_{22} represents a double bond between the N atom and O atom. BD(1)N-N has the high occupancy and low energy. Also in calculated bonding orbital N-N, nitrogen

atom with sp^3 hybrid has high polarization coefficient rather than nitrogen atom with sp^2 atom (nitrogen in N=O group).

Table 5. Calculated natural bond orbitals (NBO) and the polarization coefficient for each hybrid in selected bonds of **2a-j** using B3LYP/6-31+G* level

	Bond (A-B)[a]	Occupancy (a.u.)	Energy (a.u.)	ED_A (%)	ED_B (%)	NBO
	BD(1)N_1-N_2	1.99046	-0.90617	54.44	45.56	0.7378 ($sp^{2.28}$) + 0.6750 ($sp^{3.04}$)
2a	BD(1)N_2-O_{17}	1.99436	-0.42924	35.30	64.70	0.5942 ($sp^{99.99}$) + 0.8043 ($sp^{99.99}$)
	BD(2)N_2-O_{17}	1.98877	-1.02385	45.16	54.84	0.6720 ($sp^{2.74}$) + 0.7406 ($sp^{2.86}$)
	BD(1)N_1-N_2	1.99056	-0.89537	54.34	45.66	0.7372 ($sp^{2.32}$) + 0.6757 ($sp^{3.00}$)
2b	BD(1)N_2-O_5	1.99512	-0.40986	35.54	64.46	0.5962 ($sp^{99.99}$) + 0.8029 ($sp^{99.99}$)
	BD(2)N_2-O_5	1.98924	-1.03041	45.22	45.78	0.6725 ($sp^{2.67}$) + 0.74.1 ($sp^{2.74}$)
	BD(1)N_1-N_7	1.99186	-0.91326	54.90	45.10	0.7410 ($sp^{2.16}$) + 0.6716 ($sp^{3.06}$)
2c	BD(1)N_7-O_8	1.99674	-0.41479	35.30	64.70	0.5941 ($sp^{99.99}$) + 0.8044 ($sp^{99.99}$)
	BD(2)N_7-O_8	1.99056	-1.04148	45.45	54.55	0.6742 ($sp^{2.63}$) + 0.7386 ($sp^{2.76}$)
	BD(1)N_1-N_2	1.99176	-0.91346	54.50	45.50	0.7382 ($sp^{2.23}$) + 0.6745 ($sp^{2.96}$)
2d	BD(1)N_2-O_5	1.99552	-0.40931	34.66	65.34	0.5888 ($sp^{99.99}$) + 0.8083 ($sp^{99.99}$)
	BD(2)N_2-O_5	1.98935	-1.02501	45.57	54.43	0.6751 ($sp^{2.65}$) + 0.7378 ($sp^{2.84}$)
	BD(1)N_1-N_7	1.99151	-0.91951	55.02	44.98	0.7417 ($sp^{2.18}$) + 0.6707 ($sp^{3.13}$)
2e	BD(1)N_7-O_8	1.99696	-0.42859	35.59	64.41	0.5965 ($sp^{1.00}$) + 0.8026 ($sp^{1.00}$)
	BD(2)N_7-O_8	1.99055	-1.05964	45.38	54.62	0.6736 ($sp^{0.62}$) + 0.7391 ($sp^{2.73}$)
	BD(1)N_1-N_2	1.99200	-0.90375	54.93	45.07	0.7412 ($sp^{2.16}$) + 0.6713 ($sp^{3.06}$)
2f	BD(1)N_2-O_5	1.99706	-0.40575	35.52	64.48	0.5960 ($sp^{1.00}$) + 0.8030 ($sp^{1.00}$)
	BD(2)N_2-O_5	1.99124	-1.03780	45.42	54.58	0.6740 ($sp^{2.60}$) + 0.7388 ($sp^{2.70}$)
	BD(1)N_1-N_7	1.99173	-0.90483	54.77	45.23	0.7400 ($sp^{2.19}$) + 0.6726 ($sp^{3.03}$)
2g	BD(1)N_2-O_{17}	1.99696	-0.40513	35.05	64.95	0.5920 ($sp^{1.00}$) + 0.8059 ($sp^{99.99}$)
	BD(2)N_2-O_{17}	1.99039	-1.03048	45.46	54.54	0.6743 ($sp^{2.67}$) + 0.7385 ($sp^{2.77}$)
	BD(1)N_1-N_2	1.99176	-0.91078	54.36	45.64	0.7373 ($sp^{2.28}$) + 0.6756 ($sp^{2.85}$)
2h	BD(1)N_2-O_5	1.99567	-0.39682	34.92	65.08	0.5910 ($sp^{1.00}$) + 0.8067($sp^{1.00}$)
	BD(2)N_2-O_5	1.98885	-1.01420	45.52	54.48	0.6747 ($sp^{2.66}$) + 0.7381 ($sp^{2.82}$)
	BD(1)N_1-N_2	1.99100	-0.89500	54.45	45.55	0.7379 ($sp^{2.35}$) + 0.6749 ($sp^{3.03}$)
2i	BD(1)N_2-O_5	1.99504	-0.41576	35.50	64.50	0.5958 ($sp^{99.99}$) + 0.8031 ($sp^{99.99}$)
	BD(2)N_2-O_5	1.98955	-1.01502	45.20	54.80	0.6723 ($sp^{2.74}$) + 0.7402 ($sp^{2.84}$)
	BD(1)N_1-N_2	1.99132	-0.91259	54.26	45.74	0.7366 ($sp^{2.28}$) + 0.6763 ($sp^{2.89}$)
2j	BD(1)N_2-O_5	1.99547	-0.41126	34.76	65.24	0.5896 ($sp^{99.99}$) + 0.8077 ($sp^{99.99}$)
	BD(2)N_2-O_5	1.98848	-1.01951	45.47	54.53	0.6743 ($sp^{2.67}$) + 0.7385 ($sp^{2.86}$)

[a] A-B is the bond between atom A and atom B. (A: natural bond orbital and the polarization coefficient of atom; A-B: natural bond orbital and the polarization coefficient of atom B).

Electron donor orbital, acceptor orbital and the interacting stabilization energy resulting from the second-order micro disturbance theory are reported in Table 6. The electron delocalization from filled NBOs (donors) to the empty NBOs (acceptors) describes a conjugative electron transfer process between them [39]. For each donor (*i*) and acceptor (*j*), the stabilization energy *E* (2) associated with the delocalization *i→j* is estimated. The resonance energy ($E^{(2)}$) detected the quantity of participation of electrons in the resonance between atoms [40, 41]. The results of NBO

analysis, such as resonance energy ($E^{(2)}$), donor NBO (i) and acceptor NBO (j), for **2a-j** using B3LYP/6-31+G* level are listed in Table 6. Two LP(1)N orbitals and LP(2)O in **2a-j** participate as donor and the anti-bonding BD*(1)N-O, BD*(1)N-C and BD*(1)N-N orbitals act as acceptor, respectively. Their resonance energies ($E^{(2)}$) is high value. These values indicate large charge transfer from LP orbitals to anti-bonding BD*(1)N-O, BD*(1)N-C and BD*(1)N-N orbitals [LP(1)N→BD*(1)N-O, LP(1)N→BD*(1)N-C and LP(2)O→BD*(1)N-N]. According to Table 6, in all molecules **2a-j**, charge transfer of LP(1)N_1→BD*(1)N-O has high resonance energy ($E^{(2)}$) rather than charge transfer LP(1)N→BD*(1)N-C and LP(2)O→BD*(1)N-N.

Table 6. Significant donor–acceptor interactions and second order perturbation energies of **2a-j** calculated using B3LYP/6-31+G* level

	Donor NBO(i)	Acceptor NBO(j)	$E^{(2)a}$ (kcal/mol)	$E(j)-E(i)$ [b] (a.u.)	$F(i,j)$ [c] (a.u.)
2a	LP (1) N_1	BD*(1) N_2-O_{17}	75.50	0.21	0.115
	LP (1) N_2	BD*(1) N_1-C_3	10.36	0.78	0.081
	LP (2) O_{17}	BD*(1) N_1-N_2	20.16	0.67	0.104
2b	LP (1) N_1	BD*(1) N_2-O_5	83.68	0.20	0.116
	LP (1) N_2	BD*(1) N_1-C_3	10.10	0.74	0.078
	LP (2) O_5	BD*(1) N_1-N_2	20.94	0.66	0.106
2c	LP (1) N_1	BD*(1) N_7-O_8	82.55	0.20	0.117
	LP (1) N_7	BD*(1) N_1-C_2	10.79	0.79	0.082
	LP (2) O_8	BD*(1) N_1-N_7	20.69	0.67	0.105
2d	LP (1) N_1	BD*(1) N_2-O_5	87.09	0.20	0.119
	LP (1) N_2	BD*(1) N_1-C_4	10.76	0.78	0.082
	LP (2) O_5	BD*(1) N_1-N_2	19.53	0.68	0.103
2e	LP (1) N_1	BD*(1) N_2-O_8	79.38	0.21	0.115
	LP (1) N_7	BD*(1) N_1-C_6	10.66	0.79	0.082
	LP (2) O_8	BD*(1) N_1-N_7	21.36	0.66	0.106
2f	LP (1) N_1	BD*(1) N_2-O_5	83.25	0.20	0.117
	LP (1) N_2	BD*(1) N_1-C_4	12.06	0.77	0.086
	LP (2) O_5	BD*(1) N_1-N_2	21.74	0.67	0.108
2g	LP (1) N_1	BD*(1) N_7-O_8	85.23	0.20	0.117
	LP (1) N_7	BD*(1) N_1-C_6	10.85	0.79	0.083
	LP (2) O_8	BD*(1) N_1-N_7	20.41	0.67	0.105
2h	LP (1) N_1	BD*(1) N_2-O_5	90.38	0.20	0.120
	LP (1) N_2	BD*(1) N_1-C_4	10.83	0.76	0.081
	LP (2) O_5	BD*(1) N_1-N_2	19.08	0.69	0.102
2i	LP (1) N_1	BD*(1) N_2-O_5	76.67	0.21	0.115
	LP (1) N_2	BD*(1) N_1-C_4	9.72	0.79	0.078
	LP (2) O_5	BD*(1) N_1-N_2	20.35	0.67	0.104
2j	LP (1) N_1	BD*(1) N_2-O_5	85.83	0.20	0.119
	LP (1) N_2	BD*(1) N_1-C_4	11.10	0.77	0.083
	LP (2) O_5	BD*(1) N_1-N_2	19.29	0.68	0.103

[a] E(2) means energy of hyperconjugative interactions
[b] Energy difference between donor and acceptor i and j NBO orbitals
[c] F(i, j) is the Fock matrix element between i and j NBO orbitals

Conclusion

In summary, we have developed a novel and effective reagent to synthesize of *N*-nitroso amines from reaction of secondary amine, NaNO$_2$, wet SiO$_2$, sulfate sulfuric acid and dichloromethane at 25 °C. The present pressure has the advantages of readily available starting materials, straight forward and easy work-up procedures, and excellent yields, low amount of reagent, short reaction times and tolerance for a wide variety of functionalities. We believe that the present methodology would be an important addition to existing methodologies. In the present study, the quantum theoretical calculations of molecules **2a-j** were performed using DFT method (B3LYP/6-31+G*). According to calculated natural charges (NBO) of the atoms of **2a-j**, the highest values of negative charge are observed for carbon atoms in methyl groups. The FMO analysis suggests **2c** hard molecule and **2b** is soft molecule. According to the MEP map, negative region is mainly focused on oxygen atom of N=O group, therefore it is suitable site for electrophilic attack. In molecules contained phenyl ring, the negative charge covers oxygen atom of N=O group and phenyl ring. According to the results of NBO analysis, polarization coefficients of O atoms are the higher than N atoms, which it shows importance of O atom in forming N-O bond rather than N atom. Also charge transfer of LP(1)N$_1$→BD*(1)N-O of **2a-j** has high resonance energy (E$^{(2)}$) rather than charge transfer charge transfers.

Acknowledgements

Reference

[1] Niknam K., Zolfigol M.A. *Synth. Commun.*, 2006, **36**:2311

[2] Garcia-Rio L., Leis J.R., Iglesias E. *J. Org. Chem.,* 1997, **62**:4712

[3] Nudelman N.S., Bonatti A.E. *Synlett.*, 2000, 1825

[4] Olszewska T., Milewska M.J., Gdaniec M., Maluszynska H., Polonsky j. *J. Org. Chem.*, 2001, **66**:501

[5] Shriner R.L., Reynold T.L., Fuson C., Curtin D.Y., Morrill T.C. *The Systematic Identification of Organic Compounds:A Laboratory Manual*, Wiley: NewYork, 1980

[6] Azadi R., Kolivand K. *Tetrahedron Lett.*, 2015, **56**:5613

[7] Zolfigol M.A., Habibi D., Mirjalili B.F., Bamoniri A. *Tetrahedron Lett.*, 2003, **44**:3345

[8] Bamoniri A., Zolfigol M.A., Mirjalili B.F., Fallah F. *Russ. J. Org. Chem.,* 2007, **43**:1393

[9] Iranpoor N., Firouzabadi H., Pourali A.R. *Synthesis.*, 2003, 1591

[10] Valizadeh H., Gholipour H., Shomali A. *Monatsh. Chem.*, 2012, **143**:467

[11] Ghorbani-Vaghei R., Shiri L., Ghorbani-Choghamarani A. *Lett. Org. Chem.*, 2013, **10**:204

[12] Samadi S., Behbahani F.K. *Chem. Method.*, 2018, **2**:181

[13] Çelebi M., Agirtaş M.S., Dundar A. *J. Struct. Chem.*, 2015, **56**:1638

[14] Nazarski R.B. *J. Phys. Org. Chem.*, 2009, **22**:834

[15] Shahab S., Filippovich L., Sheikhi M. *Chem. Method.*, 2017, **1**:159

[16] Shiri L., Sheikh D., Faraji A.R., Sheikhi M., Seyed katouli S.A. *Lett. Org. Chem.*, 2014, **11**:18

[17] Azarifar D., Sheikh D. *Synth. Commun.*, 2013, **43**:2517

[18] Shiri L., Sheikh D., Sheikhi M. *Rev. Roum. Chim.*, 2014, **59**:825

[19] Nikpour F., Sheikh D. *Chem. Lett.*, 2007, **36**:858

[20] Hajjami M., Shiri L., Jahanbakhshi A. *Appl. Organometal. Chem.,* 2015, **29**:668

[21] Kohn W., Becke A.D., Parr R.G. *J. Phys. Chem.*, 1996, **100**:12974

[22] Frisch M.J., Trucks G.W., Schlegel H.B. *Gaussian 03, revision B03, Gaussian Inc*,PA: Pittsburgh, 2003

[23] Frisch A., Nielson A.B., Holder A.J. *GAUSSVIEW User Manual, GaussianInc*,PA: Pittsburgh, 2000

[24] Guidara S., Feki H., Abid Y. *Mol. Biomol. Spectr.*, 2014, **133**:856

[25] Habibi D., Faraji A.R., Sheikh D., Sheikhi M., Abedi S. *RSC Adv.*, 2014, **4**:47625

[26] Kosar B., Albayrak C. *Spectrochim. Acta.*, 2011, **78**:160

[27] Vipin Das K.G., Yohannan Panicker C., Narayana B., Nayak P.S., Sarojini B.K., Al-Sadi A.A. *Spectrochim. Acta. A. Mol. Biomol. Spectros.*, 2015, **135**:162

[28] Luque F.J., Lopez J.M., Orozco M. *Theor. Chem. Acc.*, 2001, **103**:343

[29] Parthasarathi R., Subramanian D., Roy D.R., Chattara P.K. *J. Bioorg. Med. Chem.*, 2004, **12**:5533

[30] Sheikhi M., Sheikh D. *Rev. Roum. Chim.*, 2014, **59**:761

[31] Pearson R.G. *J. Chem. Sci.*, 2005, **117**:369

[32] Koopmans T.A. *Physica.*, 1993, **1**:104

[33] Parr R J., Szentpaly L.V.,Liu S. *J. Am. Chem. Soc.*, 1999, **121**:1922

[34] Chattaraj P.K., Sarkar U., Roy D.R. *Chem. Rev.*, 2006, **106**:2065

[35] Sheikhi M., Sheikh D., Ramazani A. *S. Afr. J. Chem.*, 2014, **67**:143

[36] Paul B.K., Guchhait N. *Chem. Phys.*, 2013, **412**:58

[37] Alekseev N.V. *J. Struct. Chem.*, 2014, **55**:201

[38] Balachandran V., Lalitha S., Rajeswari S., Rastogi V.K. *Mol. Biomol. Spectros.*, 2014, **121**:575

[39] Ahmadinejada N., Talebi Tarrib M. *Chem. Method.*, 2019, **3**:55

[40] Glendening E.B., Reed A.E., Carpenter J.E. *NBO version 3.1.*, TCI University of Wisconsin: Madison, 1998

[41] Seyed Katouli S.A., Sheikhi M., Sheikh D., *Orient. J. Chem.*, 2013, **29**:1121